OPTICAL PROPERTIES OF TUNGSTEN MONOCRYSTALS

L. V. NOMEROVANNAYA, M. M. KIRILLOVA, and M. M. NOSKOV

Institute of Metal Physics, USSR Academy of Sciences

Submitted August 7, 1970

Zh. Eksp. Teor. Fiz. 60, 748–758 (February, 1971)

The frequency dispersion of the dielectric constant $\epsilon(\omega)$ of tungsten monocrystals is measured in the (110) and (100) planes and in the spectral range from 20 to $0.265\,\mu$ (0.062 to 4.9 eV). The plasma frequency of conductivity electrons is determined. Features of interband transitions are studied. Low energy conductivity spikes at energies of 0.33 and 0.40 eV are observed which are related to spin-orbit splitting of the bands near the Fermi level. The results are discussed on the basis of modern concepts about the structure of energy bands in tungsten.

THE electronic structure and Fermi surface of tungsten have been studied intensively in recent years, both experimentally and theoretically. The energy spectrum of tungsten has been calculated both relativistically[3] and non-relativistically.[1,2] By means of investigations of the de Haas–van Alphen effect,[4,5] the shape and size of the Fermi surface have been determined, and these have been in the main in accordance with relativistic calculations of the tungsten zone structure. However, there remains a small quantitative discrepancy between theory and experiment.

Optical measurements provide several important micro-characteristics of the conduction electrons—their plasma frequency Ω and the relaxation frequency γ, as well as the energy gaps between the bands in the region of allowed electronic transitions in k space.

The optical properties of bulk polycrystalline tungsten have been investigated by Roberts[6] in the 0.5–0.8-μ region, and by Lenham and Treherne[8,9] in the 0.35–20-μ region. Juenker, LeBlanc, and Martin[10] measured the reflectivity of tungsten from 0.577 to $0.05\,\mu$. We ourselves made detailed investigations on polycrystalline tungsten of 99.9% purity in the region from 0.296 to $18\,\mu$.[11]

In this paper we present the results of the first study of the optical properties of monocrystalline samples of tungsten over a wide spectral range, $0.265–20\,\mu$ (4.9–0.06 eV). The results are compared with the features of the tungsten energy spectrum.

EXPERIMENTAL PART

Samples

The samples were obtained from monocrystals of tungsten grown by the method of electron-beam zone melting. The surfaces of the samples were cut parallel to (110) and (100) planes with an accuracy of 2°, as determined by the Laue back-reflection x-ray technique. The surfaces were 15×90 mm in size.

The monocrystals were sanded with various grits and then polished electrolytically in a 1% NaOH solution at a current density of 0.4 A/cm² and temperature 24 ± 2°C for 60 min. Stainless steel was used as the cathode. In this process a layer 20 to $25\,\mu$ thick was removed. The resulting surface was free of work hardening, as proved by x rays. Schultz topograms in white

radiation were taken of the polished surfaces of crystals from which layers of 15, 20, 30, and $40\,\mu$ had been removed. They showed that even with removal of a 15–20-μ layer strains in the surface layer due to polishing were absent. At the same time the optical constants of these crystals were measured in the ir region; their values stabilized with layer removal of $t \geq 20\,\mu$. After polishing the surfaces were plane and specular.

In the process of measurement it was noted that for several hours after electropolishing, there were changes in ψ and Δ (ψ is the azimuth of "reduced" polarization, Δ is the difference in the phase shifts of the s and p components upon reflection from the sample). This seems to be due to the formation of an oxide layer on the crystal surface. The maximum change in the optical constants did not exceed 10%.

In order to eliminate the effect of the oxide layer, measurements of the optical constants were made on freshly polished samples in the three to four hours after polishing. Before each series of measurements the samples were polished anew.

Thus the surfaces of the monocrystals for optical measurement were prepared in the most careful manner.

Apparatus and Method of Measurement

The index of refraction n and the absorption coefficient k were measured by Beattie's polarimetric method[12] in an IKS-12 infrared spectrometer and an SF-4 spectrophotometer. The measurements were done at room temperature every 1.0, 2.5, 0.1, 0.05 and $0.025\,\mu$ in the spectral ranges 20–10, 10–4, 4–2, 2–1, and $1–0.4\,\mu$, respectively.

RESULTS

For each wavelength 8 to 20 series of measurements were made. The average values of n and k for the tungsten sample ($\rho(293\,\text{K})/\rho(20\,\text{K}) = 1840$) with the (110) plane are presented in the table. The rms error of the average value was 2 to 3% for n in the region 1–2μ, 3 to 4% in the region 2–18μ; for k it was 1–2% from 1 to $4\,\mu$, 2–3% from 5 to $8\,\mu$, and 4–6% in the 10–18-μ region.

Analogous measurements were made with the other sample of tungsten ($\rho(293\,\text{K})/\rho(20\,\text{K}) = 480$) with the (100) plane. The values of n and k coincided, within the limits

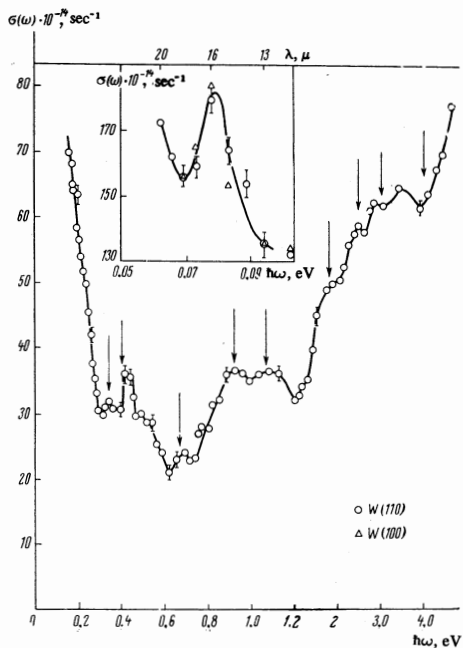| λ, μ	n	k	λ, μ	n	k	λ, μ	n	k
0.265	2.43	2.81	1.55	2.50	5.60	4.50	2.85	19.9
0.280	2.49	2.61	1.60	2.60	5.75	4.75	3.33	19.8
0.288	2.50	2.60	1.65	2.40	6.20	5.00	3.48	21.2
0.302	2.49	2.58	1.70	2.10	6.15	5.25	4.11	22.3
0.312	2.46	2.59	1.75	2.00	6.55	5.50	4.48	22.4
0.355	2.78	2.85	1.80	2.10	6.75	5.75	4.50	22.8
0.400	3.00	2.75	1.90	2.00	7.25	6.00	4.85	22.6
0.425	3.13	2.81	2.00	1.75	8.00	6.25	4.90	23.8
0.450	3.16	2.86	2.10	1.85	8.90	6.50	5.03	24.8
0.475	3.24	2.84	2.20	1.90	9.60	6.75	5.40	26.4
0.500	3.31	2.96	2.30	2.00	10.1	7.00	5.35	28.3
0.525	3.33	2.93	2.40	2.15	11.5	7.25	5.20	29.5
0.550	3.39	2.96	2.50	2.05	11.5	7.50	5.15	31.0
0.575	3.43	2.96	2.60	2.15	12.0	7.75	5.40	32.3
0.600	3.44	2.92	2.70	2.10	12.6	8.00	6.10	33.3
0.650	3.50	3.08	2.80	2.30	13.6	8.25	6.00	34.2
0.700	3.63	3.12	2.90	2.55	13.5	8.50	6.40	35.0
0.750	3.66	3.05	3.00	2.60	13.8	9.00	7.30	37.6
0.800	3.52	2.96	3.10	2.20	14.2	9.50	7.40	39.5
0.850	3.32	3.00	3.20	2.22	14.6	10.0	8.25	41.5
0.900	3.25	3.14	3.30	2.26	14.9	11.0	9.50	46.3
0.950	3.07	3.30	3.40	2.32	15.5	12.0	10.9	50.4
1.00	3.00	3.50	3.60	2.00	16.5	13.0	10.7	52.6
1.10	3.01	4.34	3.70	2.20	16.9	14.0	12.8	55.7
1.20	3.10	4.60	3.90	2.22	17.9	15.0	14.5	58.3
1.30	3.20	5.05	4.00	2.23	18.3	16.0	16.0	59.8
1.35	3.20	5.16	4.10	2.30	18.8	15.0,	15.4	60.0
1.40	3.20	5.25	4.20	2.50	19.0	17.0	15.4	61.6
1.45	3.00	5.15	4.40	2.65	19.8	18.0	16.3	63.0
1.50	2.90	5.40				19.0	16.0	66.0
						20.0	17.5	

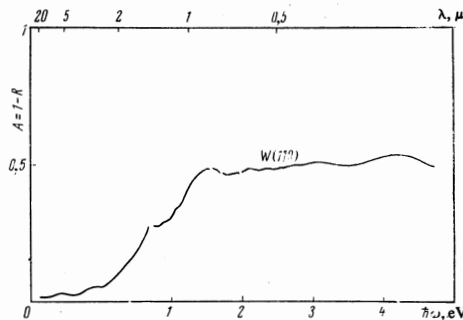FIG. 1. Conductivity $\sigma(\omega) = nk\omega/2\pi$ of tungsten.

FIG. 2. Absorptivity $A(\omega)$ of tungsten.

of error, with the data for W (110). This is not surprising, since the resistivity of both crystals at room temperature is the same, and cubic crystals with normal skin effect do not have anisotropic optical properties.

From the measured values of n and k we calculated the real $\epsilon_1(\omega)$ and imaginary $\epsilon_2(\omega)$ parts of the complex dielectric constant of tungsten, its high-frequency conductivity $\sigma(\omega)$, and the absorptivity $A(\omega)$ (Figs. 1, 2).

In analyzing the dispersive behavior of the conductivity $\sigma(\omega)$ (Fig. 1), we see that in the region $4-20\,\mu$ ($\hbar\omega = 0.3-0.062$ eV), the optical properties of tungsten are determined mainly by the mechanism of intraband acceleration of the electrons by the field of the light wave. With decreasing frequency of the field both quantities $1-\epsilon_1(\omega)$ and $\sigma(\omega)$ increase. However, in the 15 to 17-μ region there is a marked peak on the conductivity curve (Fig. 1), indicating the onset of interband transitions. The height of this peak is not great; it amounts to 15% of the general background due to the intraband acceleration. The quantity $\epsilon_1(\omega)$ also displays an anomalous behavior in this region.

Interband transitions in W begin to plan a significant role at $4.1\,\mu$ ($\hbar\omega = 0.3$ eV). This fact was noted earlier in [7] and [11].

The present results in the near infrared, visible, and ultraviolet agree well with the data of Roberts,[6] and of Juenker et al.[10] (Fig. 3). These authors prepared the surfaces of the samples by electrolytic polishing followed by a heat treatment in vacuum at 10^{-9} Torr. The agreement with [9] is not so good. In particular, the quantity $1-\epsilon_1(\omega) = 1 + k^2 - n^2$ in the 10 to 20-μ region is one-and-a-half times greater in our work, corresponding to a higher value for the absorption coefficient k of tungsten.

DISCUSSION

a) Determination of the Plasma Frequency of the Conduction Electrons

At room temperature in the transition metals the conditions for the normal skin effect are fulfilled, and
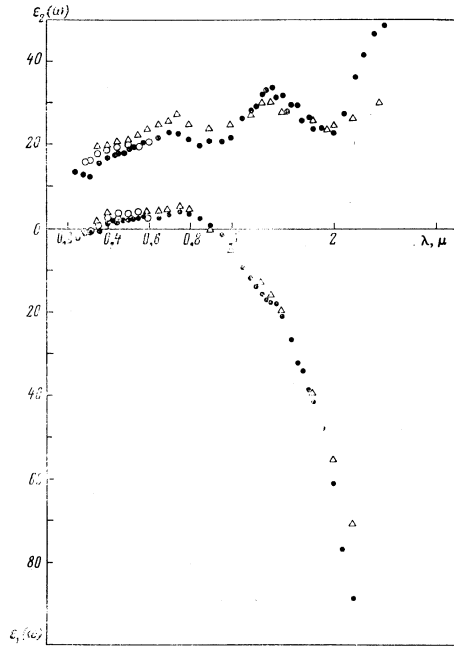
FIG. 3. Comparison of $\epsilon_1(\omega)$ and $\epsilon_2(\omega)$ for tungsten: $\triangle$—data of Roberts [6]; O—data of Juenker [10]; ●—this work, W(110).
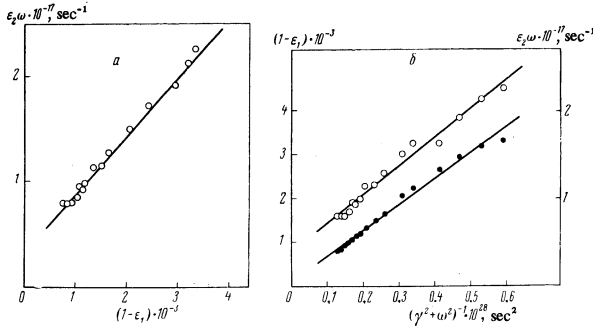

FIG. 4. a—Argand diagram for tungsten; b—dependence of light conductivity ● and dielectric constant O of tungsten on $(\omega^2 + \gamma^2)^{-1}$.

the optical properties are described by

$$\varepsilon_1(\omega) = n^2 - k^2 = 1 + \tilde{\varepsilon}_1(\omega) - \frac{\Omega^2}{\omega^2 + \gamma^2},$$
$$\varepsilon_2(\omega) = 2nk = \tilde{\varepsilon}_2(\omega) + \frac{\Omega^2 \gamma}{(\omega^2 + \gamma^2)\omega}, \quad (1)$$

where $\tilde{\varepsilon}_1(\omega)$, $\tilde{\varepsilon}_2(\omega)$ are the real and imaginary parts of the interband dielectric constant, Ω is the plasma frequency of the conduction electrons, γ is the collision frequency of the electrons, and ω is the cyclic frequency.

Let us consider the interval 7 to 14 μ, within which both $\epsilon_1(\omega)$ and $\epsilon_2(\omega)$ vary monotonically with frequency. Assuming that in this interval $\tilde{\varepsilon}_2(\omega) = 0$ and $\tilde{\varepsilon}_1(\omega) = P$, we determine the parameters Ω and γ for tungsten using the scheme set forth in [13] and Eq. (1). The slope of the straight line representing the "Argand diagram" (Fig. 4,a) gives $\gamma = 0.5 \times 10^{14}$ sec^{-1}. The slope and intercept of the line $1 - \epsilon_1(\omega)$ as a function of $(\omega^2 + \gamma^2)^{-1}$ for this value of γ yield $\Omega^2 = 59 \times 10^{30}$ sec^{-2} and P = 70. A similar result for the plasma frequency is obtained from the linear dependence of $\epsilon_2(\omega)\omega$ on $(\omega^2 + \gamma^2)^{-1}$ (Fig. 4,b).

The contribution of the interband transitions to the polarizability of tungsten in the region 14–17 μ is small. In fact, in this region P is only 1.5–7% of the intraband $\epsilon_1(\omega)$. Hence the slope of the line

$$\frac{1}{1 - \varepsilon_1(\omega)} \approx \frac{\omega^2}{\Omega^2} + \frac{\gamma^2}{\Omega^2}$$

as a function of the square of the frequency (in this case P is neglected) also gives the value $\Omega^2 = 59 \times 10^{30}$ sec^{-1}.

The line $\epsilon_2(\omega)\omega = f(\omega^2 + \gamma^2)^{-1}$ (Fig. 4,b) has a y-intercept. The presence of a nondispersive contribution to $\epsilon_2(\omega)$ is a typical feature of almost all transition 3d and 4d metals[14] and indicates the participation in the conductivity of rapidly relaxing electrons for which $\gamma^2 \gg \omega^2$. These electrons do not contribute to $\epsilon_1(\omega)$.

The least squares method was used to determine the parameters of the experimental lines.

It is known that Ω^2 is determined by the character of the spectrum and by interelectronic correlation effects. In the gas approximation for metals of cubic symmetry it is described by:[15]

$$\Omega^2 = \frac{e^2}{3\pi^2\hbar} \int v\, dS, \quad (2)$$

where v is the electron velocity on the Fermi surface and dS is an element of area of this surface. The integration is carried out over all leaves of the Fermi surface.

In the case of an arbitrary Fermi surface for area S_F, this inequality holds:

$$\int v\, dS \int \frac{dS}{v} \geqslant S_\Phi^2. \quad (3)$$

If the density of states on the Fermi level

$$G(E_\Phi) = \frac{1}{4\pi^3\hbar} \int \frac{dS}{v} \quad (4)$$

and S_F are known, we can obtain the lower value of the plasma frequency on the basis of (2)–(4).

The density of states for all leaves of the Fermi surface is determined from the experimental value of the temperature coefficient of electronic heat capacity:

$$\gamma_0 = \frac{1}{3}\pi^2 k^2 G(E_\Phi) A / d, \quad (5)$$

where k is the Boltzman constant, A is the atomic weight, and d is the density.

From the model of Sparlin and Marcus[4] the total area of the Fermi surface S_F of tungsten is 16Å^{-2}. Evaluation of S_F from the size effect gives 15.2 Å^{-2}.[16] Girvan, Gold, and Phillips,[5] refining the empirical model of the Fermi surface of W proposed by Sparlin and Marcus, gave a new value for S_F = 14.4 Å^{-2}. Using this last value for S_F, as well as A = 183.8, d = 19.3, and $\gamma_0 = 0.84 \times 10^4$ erg/mol deg^2,[17] the square of the plasma frequency in the gas approximation is calculated to be $\Omega^2 \geq 83 \times 10^{30}$ sec^{-2}. From our optical measurements $\Omega_{opt}^2 = (59 \pm 6) \times 10^{30}$ sec^{-2}. The discrepancy between the experimental values of the plasma frequency and that calculated from the gas model amounts to about 30% and, assuming correct determination of all comparable quantities (viz., Ω_{opt}^2, S_F, γ_0), characterizes the magnitude of the correlation interaction in tungsten. However, it should be realized that the values of Ω_{opt}^2 may be somewhat too low, since at room temperature
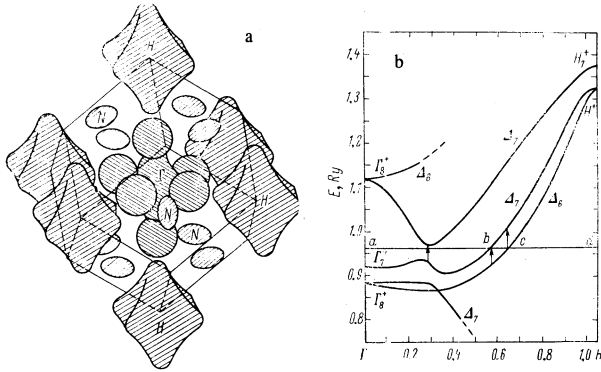
FIG. 5. a—Fermi surface of tungsten; b—relativistic spectrum of tungsten along the ΓH-direction. [19] The arrows indicate the low-energy gap in the spectrum.

not all groups of carriers may be represented in charge transfer phenomena. Besides, in our measurements we did not get into the spectral interval where interband transitions would be completely absent, and this could affect the evaluation of Ω^2_{opt}. Finally, the quantity S_F also requires refinement. For all these reasons we cannot in this case attribute the discrepancy solely to correlation effects.

b) Interband Transitions

In the region of interband electronic transitions the character of the dispersion of the high-frequency conductivity $\sigma(\omega)$ depends essentially on the structure of the energy bands lying in the immediate vicinity of the Fermi surface, as well as a few electron volts above and below it.

Theoretical and experimental investigations have shown that the two lowest energy bands in W are completely occupied (two electrons per band), whereas the third and fourth are partially filled and are the conduction bands. The Fermi surface of tungsten is shown in Fig. 5,a. In the center of the Brillouin zone (BZ) there is an electron surface of the fourth band (electronic "jack"), consisting of a central octahedral body and sphere-like protuberances. The hole surface of the third band consists of octahedral bodies ("octahedra"), localized in nodes of the BZ and small ellipsoids lying in face centers. It is also known that in the energy spectrum of tungsten there are two low-energy gaps between bands 3–4 and 4–5, the magnitude of which, according to calculations of Mattheiss and Watson[18] and Loucks,[19] span about 0.4–0.5 eV (Fig. 5,b). The fifth band in tungsten is not occupied and is above the Fermi level.

The magnitude of the energy gap between corresponding bands in the zone spectrum determines the threshold of optical absorption of the metal assuming that the transitions of electrons from occupied states to free ones of overlying bands occur with conservation of the quasi-momentum $\hbar k$.

Consider the data on the optical abosrption in the low-energy region of the spectrum (0.06–1 eV). The interband transitions give the predominant contribution to the conductivity of tungsten beginning with energy 0.3 eV (Fig. 1). Features are noted on the $\sigma(\omega)$ curve at ~0.33 and 0.4 eV.

An examination of the dispersion curves $E(k)$ for the third, fourth and fifth bands near the Fermi level (Fig. 5,b) and allowance for the selection rules for interband transitions reveal that at energies ~0.3–0.4 eV transitions between the fourth and fifth bands go in a very limited volume of the BZ and consequently give a less important contribution to the optical absorption than transitions between the third and fourth bands. Based on this we connect the weak feature in $\sigma(\omega)$ with the beginning of transitions between the fourth and fifth level and the strong one at 0.4 eV with the onset of transitions between the third and fourth bands ("jack"–octahedron). The conclusion is that the energy gaps corresponding to spin-orbit splitting of the bands in W span 0.33 and 0.4 eV according to the optical data.

However, there is still another feature on the $\sigma(\omega)$ curve in the region $\hbar\omega \sim 0.08$ eV (Fig. 1), the origin of which does not find explanation in the direct-transition model. It remains to assume that its manifestation in the optical spectrum is associated with direct transitions between the third and fourth bands, e.g., close to the point of symmetry G (Fig. 4,c of [11]). Only temperature measurements can settle this.

After a small but distinct absorption band in the interval 0.6–1.2 eV, in which there are weak features at 0.67, 0.92, and 1.07 eV, a broad absorption band begins in tungsten. This band arises because of many transitions between different bands (1–3, 4, 5, 6; 2–3, 4, 5, 6; 3–4, 5, 6; 4–5, 6). Peaks, with steps on them, are clearly seen at 1.7, 2.5, 3.1, and 4.0 eV, the appearance of which is associated with transitions of electrons close to singular points of the BZ, where $\nabla_k E_{ll'} = E_{l'}(k) - E_l(k)$. We shall not do a detailed analysis of the optical absorption spectrum, since we do not have the numerical values of $E(k)$ from the relativistic calculation.[3]

Using the parameters found above, $\Omega^2 = 59 \times 10^{30}$ sec^{-2}, $\gamma = 0.5 \times 10^{14}$ sec^{-1}, we get from the $\sigma(\omega)$ curve the contribution of the accelerating mechanism, which is described by

$$\sigma(\omega) = \frac{1}{4\pi} \frac{\Omega^2 \gamma}{(\omega^2 + \gamma^2)}.$$

Below in Fig. 7 curve 2 pertains to the interband conductivity of W, supplemented by data of [10]. In the low-energy region $0.3 \leq \hbar\omega \leq 1$ eV the values of $\tilde{\sigma}(\omega)$ are somewhat too high by virtue of some participation in the conductivity of rapidly relaxing electrons,[14] the contribution of which to $\sigma_{exp}(\omega)$ in this region we cannot take into account with accuracy. When $\hbar\omega \geq 1$ eV the phenomena of electron transfer give a negligibly small contribution to $\sigma(\omega)$. In this region $n \geq k$ and the curve $\epsilon_1(\omega)$ passes through zero twice at 1.33 and 3.2 eV.

The total width of the energy band in tungsten corresponding to the distance from the bottom of the first band to the Fermi level is, according to Loucks,[2] 7.5 eV in the nonrelativistic calculation and 10.3 in the relativistic.[3] From the same data, the width of the band in molybdenum is 7.4 eV. Broadening of the energy bands with increase of relativistic effects should be manifested in the increase of the width of the fundamental band of optical absorption in the series of metals Cr, Mo, and W. This regularity does actually occur. According to [10,20,21] and the present work, the width
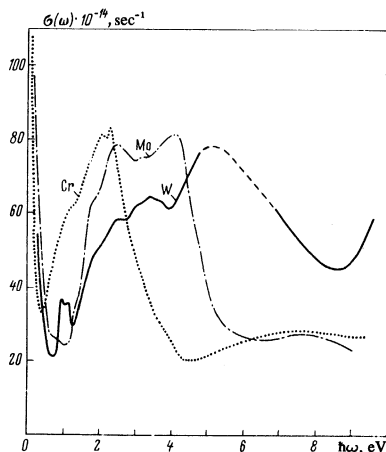
FIG. 6. Comparison of the width of the fundamental optical absorption band in chromium, [20] molybdenum, [21] and tungsten (data of this work and [10]).
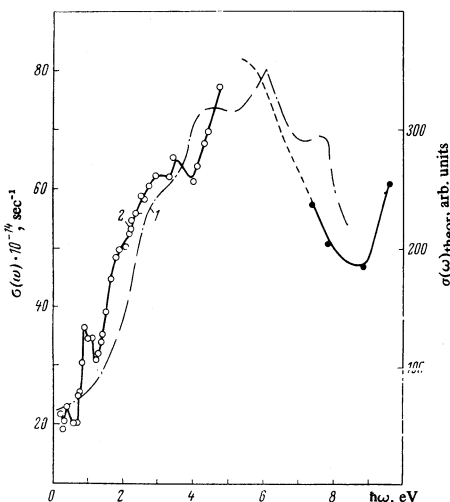

FIG. 7. Curve 1—dispersion of the conductivity of tungsten, calculated from the density of states. [1] Curve 2—experimental interband conductivity of tungsten $\tilde{\sigma}(\omega)$ according to data of this work O and [10] (●).

of the fundamental absorption band is $\sim$4 eV in chromium, $\sim$6 eV in molybdenum, and $\sim$9 eV in tungsten (Fig. 6).

We calculate the interband conductivity of tungsten using the curve of density of states obtained by Mattheiss[11] and the formula of Berglund and Spicer:[22]

$$\tilde{\sigma}_{ll'}(\omega) = \frac{M}{\omega} \int_{E_F}^{E_F + \hbar\omega} G_l(E - \hbar\omega)\, G_{l'}(E)\, dE, \qquad (6)$$

where G_l and $G_{l'}$ are the densities of states of the occupied and free bands, E_F is the Fermi level. The coefficient M, which determines the transition probabilities, is assumed constant in the first approximation. The graph of $\tilde{\sigma}_{ll'}(\omega)$ in arbitrary units obtained by numerical integration is in Fig. 7 (curve 1).[1] Calculation

---

1)The density of states obtained with potential V_2 was used. In this case Mattheiss [1] obtained results close to Loucks' relativistic calculations. [3]

from (6) predicts the existence of an absorption band in the interval 1–9 eV. This conclusion of the theory is confirmed by experimental data.

We see, therefore, that the optical properties of tungsten as a whole confirm contemporary ideas about its zone structure. In future we shall carry out temperature measurements on tungsten monocrystals; these will help refine the pattern of its interband transitions as well as evaluate the relative importance of direct and indirect transitions in the formation of the optical absorption spectrum. This will permit a more careful correlation of the optical characteristics with the features of the energy spectrum.

We thank N. V. Belova for doing the x-ray investigations and V. P. Dyakina for measuring the electrical resistance of the crystals.

[1] L. F. Matheiss, Phys. Rev. **139A**, 1893 (1965).

[2] T. L. Loucks, Phys. Rev. **139**, 1181 (1965).

[3] T. L. Loucks, Phys. Rev. **143**, 506 (1966).

[4] D. M. Sparlin and J. A. Marcus, Phys. Rev. **144**, 484 (1966).

[5] R. F. Girvan, A. V. Gold, and R. A. Phillips, J. Phys. Chem. Solids **29**, 1485 (1969).

[6] S. Roberts, Phys. Rev. **114**, 104 (1959).

[7] I. E. Leksina and N. V. Penkina, Fiz. Metal. Metalloved. **22**, 264 (1966).

[8] A. P. Lenham and D. M. Treherne, Optical Properties and Electronic Structure of Metals and Alloys, Amsterdam, 1966, p. 196.

[9] [Not in original].

[10] D. W. Juenker, L. J. LeBlanc, and C. R. Martin, J. Opt. Soc. Am. **58**, 164 (1968).

[11] L. V. Nomerovannaya, M. M. Noskov, M. M. Kirillova, G. A. Bolotin, and V. M. Maevskiĭ, Doklady simpoziuma po élektronnoĭ strukture perekhodnykh metallov i splavov (Reports of the Symposium on the Electronic Structure of Transition Metals and Alloys), Kiev, 1970.

[12] J. R. Beattie, Phil. Mag. **46**, 235 (1955); Physica **23**, 898 (1957).

[13] M. M. Noskov, Preprint, Institute of Metal Physics, Academy of Sciences, USSR, 1970.

[14] M. M. Kirillova and B. A. Charikov, Opt. Spektrosk. **17**, 254 (1964) [Opt. Spectrosc. **17**, 134 (1964)].

[15] M. I. Kaganov and V. V. Slezov, Zh. Eksp. Teor. Fiz. **32**, 1496 (1957) [Sov. Phys.-JETP **5**, 1216 (1957)].

[16] V. E. Startsev, N. V. Volkenshteĭn, and G. A. Nikitina, Fiz. Metal. Metalloved. **26**, 261 (1968).

[17] T. H. Geball, Rev. Mod. Phys. **36**, 134 (1964).

[18] L. F. Mattheiss and R. E. Watson, Phys. Rev. **138**, 526 (1964).

[19] T. L. Loucks, Phys. Rev. Lett. **14**, 693 (1965).

[20] M. M. Kirillova and M. M. Noskov, Fiz. Metal. Metalloved. **26**, 952 (1968).

[21] M. M. Kirillova, M. M. Bolotin, and V. M. Maevskiĭ, Fiz. Metal. Metalloved. **24**, 25 (1967).

[22] C. N. Berglund and W. E. Spicer, Phys. Rev. **136A**, 1044 (1964).

Translated by L. M. Matarrese
81